Supporting Information for

Sintering Rate and Mechanism of TiO_2 Nanoparticles by Molecular Dynamics

B. Buesser, A. Gröhn and S.E. Pratsinis*
Particle Technology Laboratory, Institute of Process Engineering
Department of Mechanical and Process Engineering
ETH Zurich, 8092 Zürich, Switzerland

Validation. Figure SI1 shows the calculated total energy of equilibrated rutile TiO_2 nanoparticles (open symbols) with diameter $d_{p,0}$ = 2 (triangles), 2.8 (circles) and 3 nm (squares) as function of temperature along with the simulations of Collins *et al.*[1] for d = 2.8 nm (filled circles). The energy of the $d_{p,0}$ = 2.8 nm particle calculated here is in agreement with Collins *et al.*[1]. Decreasing the particle size to $d_{p,0}$ = 2 nm leads to a small step in the total energy. This marks the transition temperature between solid- and liquid-like particles. The small size of this step indicates that the transition between liquid and solid is small explaining the liquid-like behavior of such particles (Figure 4). Increasing the particle size shifts this step to higher temperatures (2300 K for 2.8 nm and 2700 K for 3 nm), higher than the melting temperature of bulk TiO_2 in agreement with Koparde and Cummings[2].

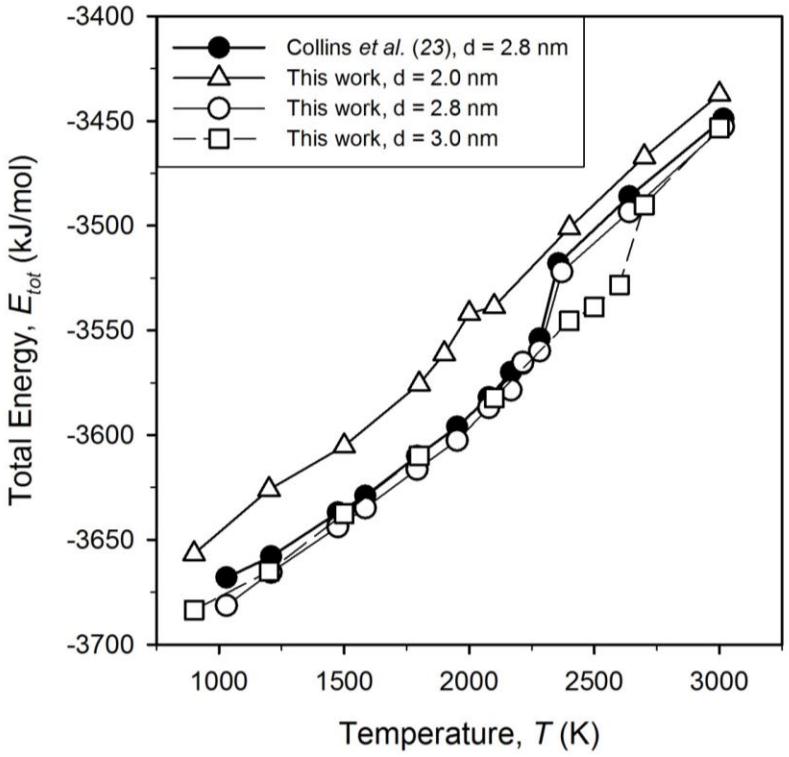

Figure SI1 The total energy of equilibrated rutile TiO_2 nanoparticles with initial diameter $d_{p,0}$ = 2.8 nm (1245 ions) of Collins *et al.*[1] (filled circles) compared with this work (open symbols) as a function of temperature.

Different Initial Particle Orientations. Figure SI2 shows that different initial particle orientations (right particle is rotated by 0 (black), 90 (red), 180 (pink) and 270° (green)) lead to slightly different evolution of surface area during all stages of sintering, but all are close to each other ($d_{p,0}$ = 3 nm and T = 1800 K). The evolution for 0° (red line) deviates slightly more than the rest but it also converges with the others at the end. The average of these four simulations is shown here and in Figure 4 (dash-dot line). The bond order parameters Q_4, W_4 and W_6 for oxygen and titanium ions in the present nanoparticles were calculated following Steinhardt *et al.*[3] with the source code of Wang *et al.*[4]. It was found that the final coalesced TiO_2 nanoparticle remained in the rutile phase as the initial ones in agreement with Koparde and Cummings[5].

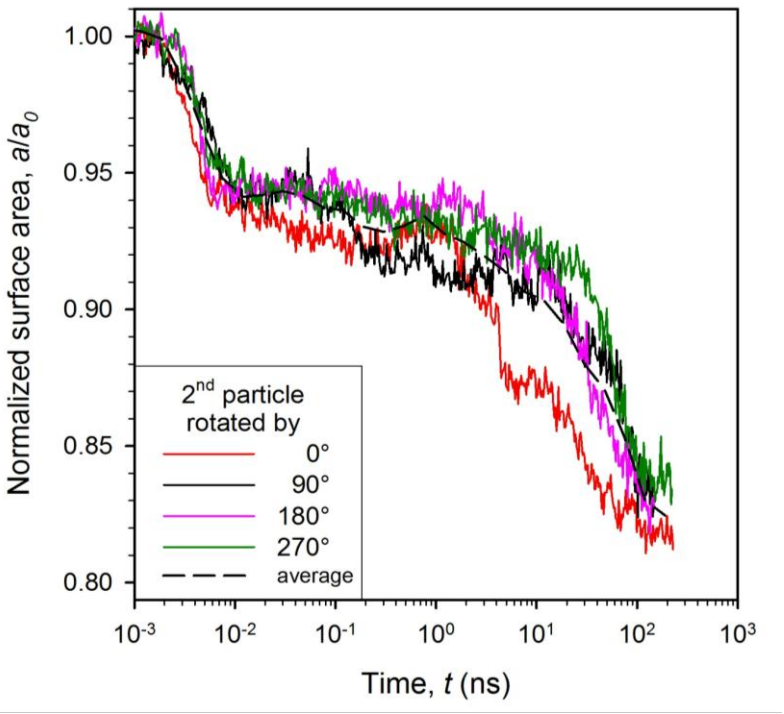

Figure SI2 Evolution of normalized surface area for two rutile TiO_2 particles undergoing sintering with $d_{p,0}$ = 3 nm at conserved T = 1800K where the right particle is rotated by 0 (red), 90 (black), 180 (pink) and 270° (green) along with their average (dashed line).

Influence of temperature on Sintering. Figure SI3 shows the average of four evolutions of normalized surface area a/a_0 for two TiO_2 nanoparticles undergoing sintering with initial diameter $d_{p,0}$ = 2.5 nm as in Fig. 4 at T = 1500 (dotted line), 1600 (dash-dot), 1700 (dashed) and 1800 K (solid). The horizontal line defines again the excess surface area reduction by 67 % as discussed in the paper. Increasing the temperature leads to shorter characteristic sintering times and therefore faster sintering in agreement with experiments[6]. Note that the initial stage of sintering (adhesion) does not depend on temperature so all evolutions are clustered together because adhesion depends mostly on particle diameter for solid particles.

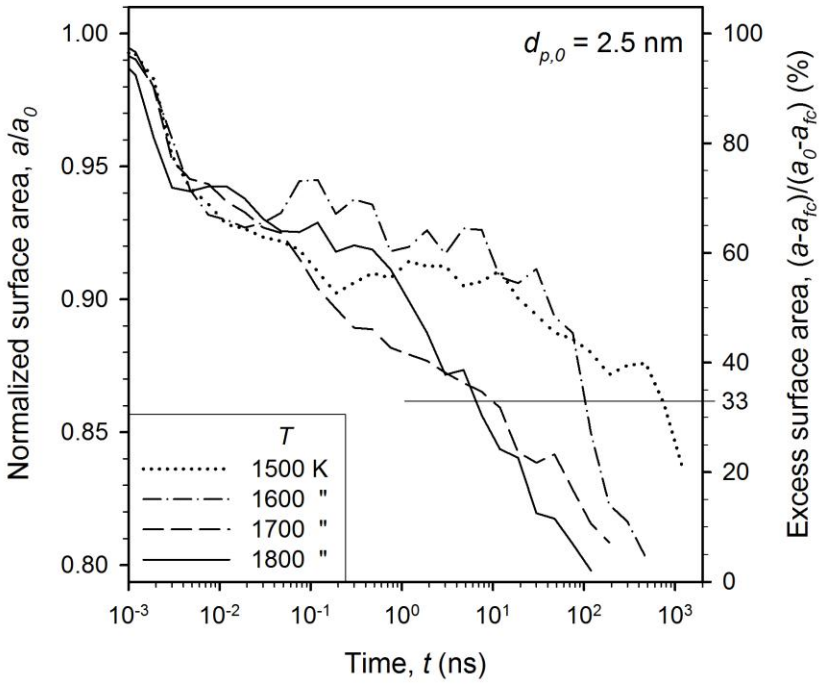

Figure SI3 Evolution of the normalized surface area of two TiO_2 nanoparticles undergoing sintering with initial diameter $d_{p,0}$ = 2.5 nm at conserved temperatures T = 1500, 1600, 1700 and 1800 K. The thin horizontal line where the excess surface area (right axis) has decreased by 67% defines the MD-obtained characteristic sintering times τ in Fig. 6 (circles).

References

(1) Collins, D. R.; Smith, W.; Harrison, N. M.; Forester, T. R. *J. Mater. Chem.* **1996**, *6*, 1385.

(2) Koparde, V. N.; Cummings, P. T. *J. Nanopart. Res.* **2008**, *10*, 1169.

(3) Steinhardt, P. J.; Nelson, D. R.; Ronchetti, M. *Phys. Rev. B* **1983**, *28*, 784.

(4) Wang, Y.; Teitel, S.; Dellago, C. *J. Chem. Phys.* **2005**, *122*, 214722.

(5) Koparde, V. N.; Cummings, P. T. *ACS Nano* **2008**, *2*, 1620.

(6) Seto, T.; Shimada, M.; Okuyama, K. *Aerosol Sci. Technol.* **1995**, *23*, 183.